Chapter 16

Laser Microbeam Targeting of Single Nerve Axons in Cell Culture

Nicholas Hyun, Linda Z. Shi, and Michael W. Berns

Abstract

By focusing a laser with short pulses to a diffraction-limited spot, single nerve axons can be precisely targeted and injured. Subsequent repair can be analyzed using various imaging and biochemical techniques to understand the repair process. In this chapter, we will describe a robotic laser microscope system used to injure nerve axons while simultaneously observing repair using phase and fluorescence microscopy. We provide procedures for controlled laser targeting and an experimental approach for studying axonal repair in embryonic rat hippocampus neurons.

Key words Ablation, Axotomy, Hippocampus, Laser, Neurons, Repair, Targeting

1 Introduction

Neuronal growth cones are specialized motile structures that react to environmental cues to guide nerve growth. The repair and reassembly of the growth cone after injury is crucial in the process of nerve regeneration and is an important step in driving axonal growth to reconnect with its target. Nerves with incomplete growth cone regeneration often exhibit dystrophic end bulbs which are markers for degenerating axons [1, 2]. The regeneration of a new growth cone involves many intracellular processes including proteolytic events, cytoskeletal rearrangement, and regulated transport of repair materials [3]. Although progress has been made in identifying causes for abnormal regeneration, additional novel ways to study nerve repair and regeneration following injury can have a significant impact on our understanding of the process.

To investigate the role of growth cones in nerve repair and regeneration, we have developed a system that can locally damage axons while simultaneously observing the repair process in real time using phase and fluorescence microscopy. By focusing a short-pulsed picosecond (ps) laser beam to a diffraction-limited spot, individual axons in cell cultures can be manipulated without dam-

Laura Lossi and Adalberto Merighi (eds.), *Neuronal Cell Death: Methods and Protocols*, Methods in Molecular Biology, vol. 1254, DOI 10.1007/978-1-4939-2152-2_16,

aging adjacent cells. The laser microscope system uses a 532 nm ps laser to partially damage (sub-axotomy) hippocampus neurons. We can then study the growth cone response to the damage. Previous preliminary studies on goldfish retinal ganglion cells in culture have shown this approach to be feasible [4, 5]. In the following sections, we will highlight key steps in using a laser ablation approach for neuron repair studies in embryonic rat hippocampus. This approach can be applied to nerve cells from other sources as well.

2 Materials

2.1 Cell Culture

1. 35 mm imaging dishes (MatTek, Ashland, MA).
2. 45×50 mm microscope cover glass (Fisherbrand, Waltham, MA).
3. 70× 50 microscope cover glass (Fisherbrand, Waltham, MA).
4. Poly-L-Lysine (Sigma-Aldrich, St. Louis, MO).
5. Culture grade water (Sigma-Aldrich).
6. Embryonic day (E) 17–18 rat embryos.
7. Fetal Bovine Serum (FBS, Life Technologies™).
8. Hanks' Balanced Salt Solution (HBSS, Life Technologies™).
9. HEPES (Life Technologies™).
10. Penicillin Streptomycin (Life Technologies).
11. 1× Neurobasal (Life Technologies™).
12. 50× B27 (Life Technologies™).
13. Glutamax (Life Technologies™).
14. OkoLab stage incubator (OkoLab, Napoli, Italy).

2.2 RoboLase: Optical Design and Hardware

Overview: Neuronal repair studies were performed using a robotic laser microscope system (RoboLase) consisting of an ablation laser, external optics to direct the laser path into the microscope, an inverted microscope with a motorized stage, CCD cameras, and Labview-based software to control the optical components as well as phase and fluorescence imaging [6]. Various optical designs can achieve similar results. We will describe our optical system and outline key components necessary for controlled laser ablation (sub-axotomy or axotomy) (Fig. 1).

2.2.1 Individual Components

1. 532 nm picosecond laser (VDGD2000-80-HM532 Spectra-Physics, Mountain View, CA).
2. Fast scanning mirror (FSM-200-01, Newport Corp, Irvine, CA).
3. Polarizers (CLPA-12.0-425-575, CVI laser, LLC, Albuquerque, NM).
4. Mechanical shutters (Vincent Associates, Rochester, NY).

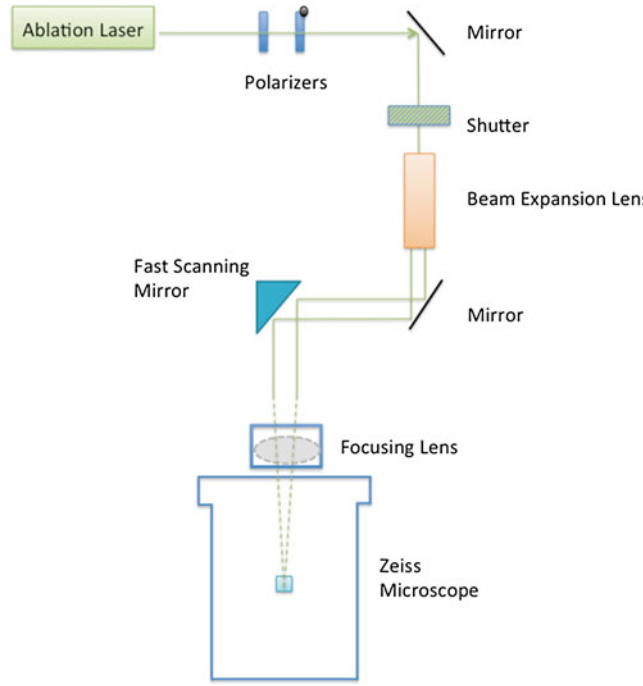

Fig. 1 Schematic of the optical hardware to direct the laser into the microscope system

5. 63×, phase III, Na1.4 oil emersion Plan-Apochromat objective (Carl Zeiss Microscopy GmbH, Jena, Germany) for neuronal ablation.
6. Beam expander lens (2–8×, 633/780/803 nm correction, Rodenstock, Germany).
7. Zeiss axiovert 200 M microscope (Carl Zeiss) with motorized objective turret, reflector turret, fluorescence filter cubes, condenser turret, halogen lamp shuttering with intensity control, mercury arc lamp shutter, camera port selection, objective focus with parfocal switching between objectives.
8. Hamamatsu camera (c4742-80-12AG, Hamamatsu Photonics, K.K., Hamamtsu, Japan).
9. Mirrors (Y2-1025-45-S, CVI Laser LLC).
10. Rotary mount (Newport Corp).
11. Photometer (Newport Corp).
12. X-Y stepper stage (Ludl Electronic Products Hawthorne, NY).
13. Stepper motion controller (National Instruments, Austin, TX).
14. MID-7604 power drive (National Instruments)
15. Computer (AlienWare Corp, Intel® Core™ 2CPU, 2.67 GHz, 2.75 GB of RAM).
16. Labview software (National Instruments).

2.2.2 External Laser Optics and Hardware

1. The ablation laser (**item 1** in Subheading 2.2.1) is a diode-pumped Vanguard Nd:YVO_4 second harmonic generator (SHG) 532 nm laser light linearly polarized with 100:1 purity, 76 MHz repetition rate, 12 ps pulse duration, and 2 W average power. *See* **Note 1**.
2. The glan linear polarizer (**item 3** in Subheading 2.2.1) is positioned after the ablation laser to increase the laser beam polarization purity.
3. The laser beam next passes through a second polarizer mounted in a rotary mount, which controls the amount of laser power and energy entering the microscope. The motorized mount (**item 10** in Subheading 2.2.1) can rotate the second polarizer to its vertical position for maximum transmission (95 %) or to its horizontal position for minimum transmission below the damage threshold of biological samples. The rotary mount is controlled through the motion controller (**item 13** in Subheading 2.2.1) in the PXI chassis [8].
4. A mechanical shutter (**item 4** in Subheading 2.2.1) with a 30 ms duty cycle gates the main laser beam resulting in a 30 ms burst of pulses that enters the microscope. The number of pulses is calculated based on the pulse rate of the laser [6, 7].
5. The laser beam passes through an adjustable-beam expander (2–8×, 633/780/803 nm correction) (**item 6** in Subheading 2.2.1) and is lowered to a height just above the optical table by using additional mirrors and mirror mounts.
6. A dual-axis fast scanning mirror (**item 2** in Subheading 2.2.1) is used to steer the laser beam at an imaged plane conjugate to the back focal plane of the microscope objective.
7. Neurons are mounted on a X-Y stepper stage (**item 12** in Subheading 2.2.1) controlled with a stepper motion controller (**item 13** in Subheading 2.2.1) and a power drive (**item 14** in Subheading 2.2.1).
8. The ORCA camera (**item 8** in Subheading 2.2.1) is linked to the system with a controller and a DCAMPI driver with Hammatsu's video Capture library for LabView.

2.3 RoboLase: Software

The software used to control the microscope, cameras, and external light paths is programmed in the LabVIEW language. The RoboLase software also manages image and measurement file storage. The "Front panel" software was designed to provide a user-friendly interface capable of meeting the demands of single cell manipulation (Fig. 2). A detailed description of the RoboLase Software has been published [8].

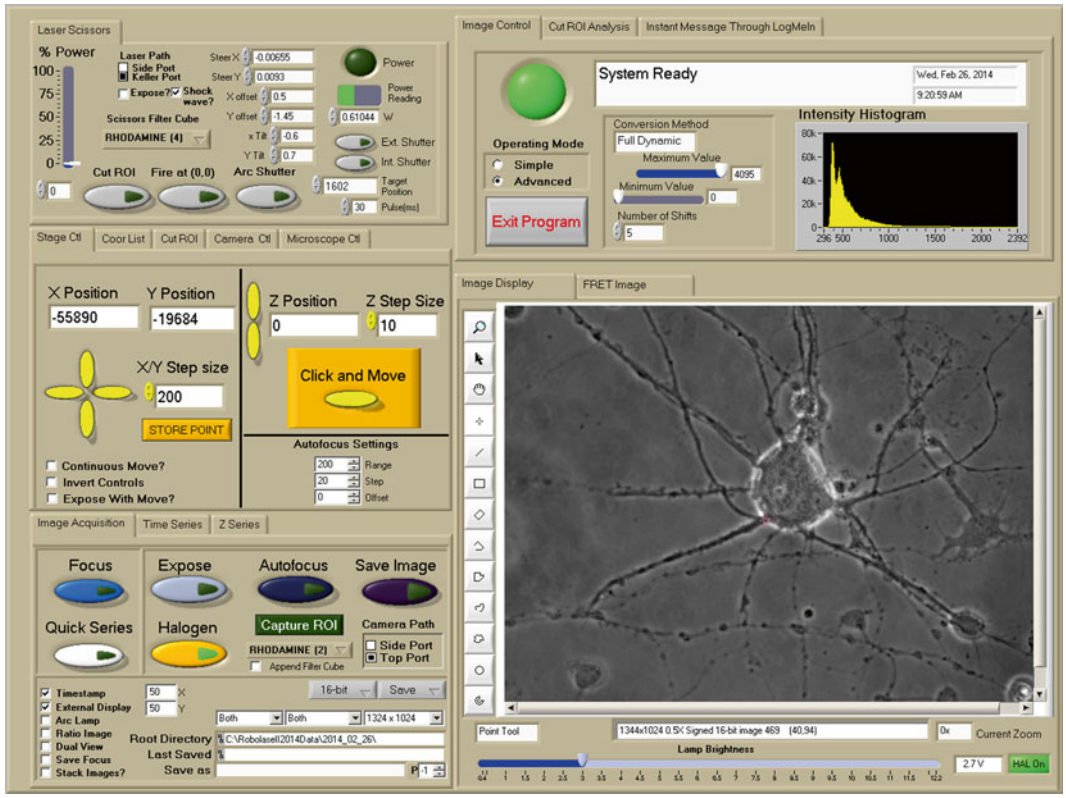

Fig. 2 Screen shot of the LabView RoboLase interface system to control laser ablation

3 Methods

3.1 Primary Nerve Cell Preparation

3.1.1 Coating Coverslips

1. Coat 35 mm imaging cell culture dishes with 250 µL of 0.2 mg/mL Poly-L-Lysine. Set dishes in incubator for 3 h or let dishes sit overnight at room temperature.
2. Aspirate Poly-L-Lysine solution and washout coating solution using culture grade water. Allow water to sit for 10 min before aspirating. Repeat 3 times. Let coated dishes dry in sterile hood before plating cells.

3.1.2 Dissection

1. Dissect hippocampal neurons from E17 to 18 rats in HBSS containing 10 mM HEPES and 1 % penicillin/streptomycin.
2. Plate them onto coated Poly-L-Lysine dishes into plating media containing Neurobasal, 2 % B27, 1 % Glutamax and 5 % FBS. *See* **Note 2**.

3. Replace 2/3 of the plating media to maintenance media containing Neurobasal, 2 % B27 and 1 % Glutamax the day after dissection.
4. Replace 2/3 of maintenance media every 2–3 days.

3.2 Laser Alignment and Targeting

3.2.1 Laser Alignment

Overview: Laser alignment is a critical step to ensure accurate and repeatable laser ablation. Alignment consists of optimizing laser profile shape and maximizing the amount of collimated light at the back aperture of the objective. When aligning the laser, remove all unnecessary personnel from the room and wear appropriate eyewear. Perform alignment tasks at the lowest power level possible.

1. Place a targeting bulls-eye at the back aperture of objective in an open turret. Place an additional targeting bulls-eye directly perpendicular to the back aperture on the ceiling 5–10 ft. above the microscope (Fig. 3).
2. Fill the back aperture of the objective by adjusting the focusing lenses and mirrors to maximize laser intensity to the center of the bulls-eye. *See* **Note 3**.
3. Align the laser to the targeting bulls-eye on the ceiling by adjusting the steering mirrors. After centering the beam on the ceiling bulls-eye, recheck the back aperture bulls-eye to insure the beam is still centered. If not, realign the beam on the back aperture and ceiling bulls-eyes with incremental adjustments. Repeat the process until both are centered. The back aperture alignment is more critical than the ceiling targeting. This alignment procedure insures that the laser beam is coming through the microscope at a perpendicular angle rather than at an angle that will result in uneven energy distribution in the focal spot and an irregular shaped focal spot in the optical field.

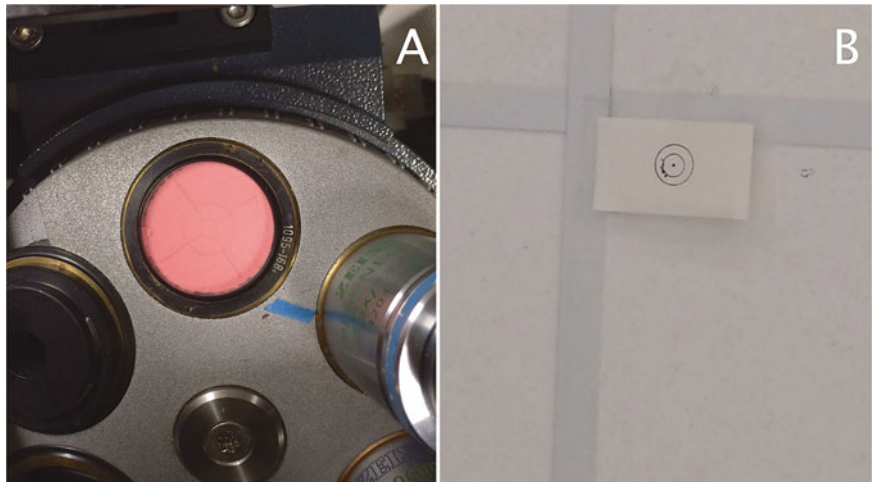

Fig. 3 Bulls-eye targets placed at the (**a**) back aperture of the objective and the (**b**) ceiling for laser alignment

3.2.2 Laser Power Measurement

Overview: The amount of laser power entering the microscope is controlled using a polarizer in a rotatory mount. By rotating the angle of the polarizer, the transmission of the laser passing through the polarizer and into the microscope can be precisely controlled. Calibrating the laser power versus polarizer position is critical for controlled and repeatable laser ablation experiments.

Laser power measurements are also important for calculating the energy and power in the focal spot used to damage axons. As the laser passes through the optical hardware and objective lens, some of the beam power is attenuated. To determine the laser power at the focus spot of the objective, the transmittance of the objective is multiplied by the laser power measured at the back aperture. A modified dual objective method is used to calculate the transmission of the objective (*see below and* 9).

1. Manually open mechanical shutter controller switch in laser path and turn on laser. Make sure the microscope port is changed to the base port such that the laser can enter the back aperture of the objective.
2. Measure the laser power at the back aperture of the objective with a photometer. This value is the power entering the objective (P_{in}). Make sure the photometer is set to the correct wavelength and is aligned to provide maximum intensity.
3. Place two objectives (A and B) coaxially such that the lenses are facing each other with emersion oil and a glass coverslip in-between the objectives (Fig. 4).
4. Align the combined objectives in the X, Y, Z planes to maximize the amount of laser light exiting the back aperture of objective B (P_{out}) and measure the power using a photometer.
5. The transmission of the combined objectives is calculated using the following equations:

$$T_1 = \frac{P_{\text{out}}}{P_{\text{in}}} \tag{1}$$

$$T_1 = T_{\text{A}} \times T_{\text{B}} \tag{2}$$

where the T_{A} and T_{B} equal the transmission of objective A and B respectively.

6. To solve for T_{A} and T_{B} a third objective is needed. Using Eqs. (1) and (2), the following equations can be used to solve the transmittance for three objectives (A, B, and C)

$$T_{\text{A}}^2 \times T_{\text{B}}^2 \times T_{\text{C}}^2 = T_1 \times T_2 \times T_3 \tag{3}$$

$$T_{\text{A}} \times T_{\text{B}} \times T_{\text{C}} = \sqrt{T_1 \times T_2 \times T_3} \tag{4}$$

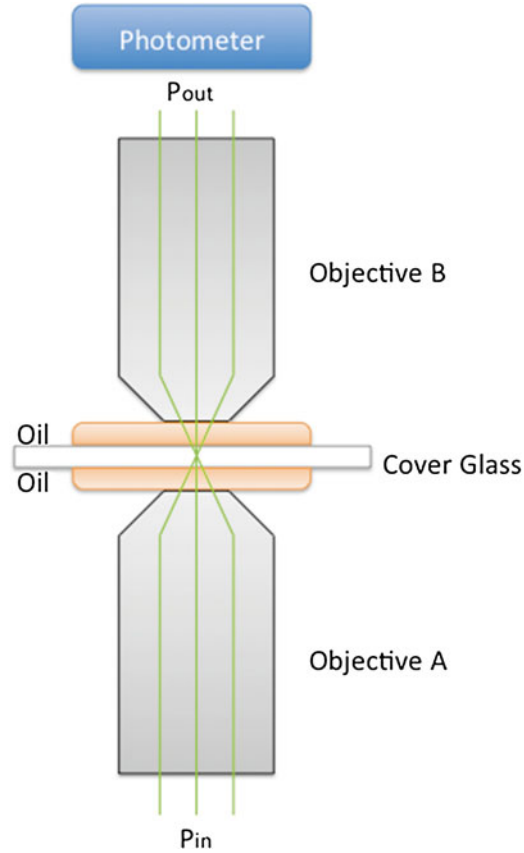

Fig. 4 Schematic of the dual-objective method

$$T_{\mathrm{A}} = \frac{\sqrt{T_1 \times T_2 \times T_3}}{T_2} \tag{5}$$

$$T_{\mathrm{B}} = \frac{\sqrt{T_1 \times T_2 \times T_3}}{T_3} \tag{6}$$

$$T_{\mathrm{C}} = \frac{\sqrt{T_1 \times T_2 \times T_3}}{T_1} \tag{7}$$

The focus spot power equals (P_{in}) times the transmittance of the objective. *See* **Note 4** [10].

7. Repeat **step 2** at different polarizer positions to calibrate the laser power vs. polarizer position. *See* **Note 5**.

3.2.3 Laser Dosage Calculation

1. Assuming X is the power reading that creates the expected laser damage, the energy per pulse is equal to

$$\frac{X \times \text{Objective transmission}}{\text{Laser repetition rate}}.$$

2. The total laser dosage is energy per pulse × number of pulses per shot × number of spots in the damage.

3.3 Laser Targeting

Overview: After laser alignment and power measurements, the accuracy of the laser must be calibrated by firing at a uniform pigmented target. We use dried human red blood cells (RBC) that have been spread on a 45 × 50 mm cover glass. *See* **Note 6**.

A good RBC smear (*see* the cell images in Fig. 5) mounted and inverted on a 70 × 50 mm microscope slide can be used for over a year.

1. Open and run the RoboLase software. Load prepared RBC cells on microscope stage. *See* **Note 7**.
2. Set the power at a relatively high output by moving the slider for laser power in the upper left "Laser Scissors".
3. Click the "point" cursor on the side bar of the image and draw a point underneath the crosshair in the acquired image as shown in Fig. 2.

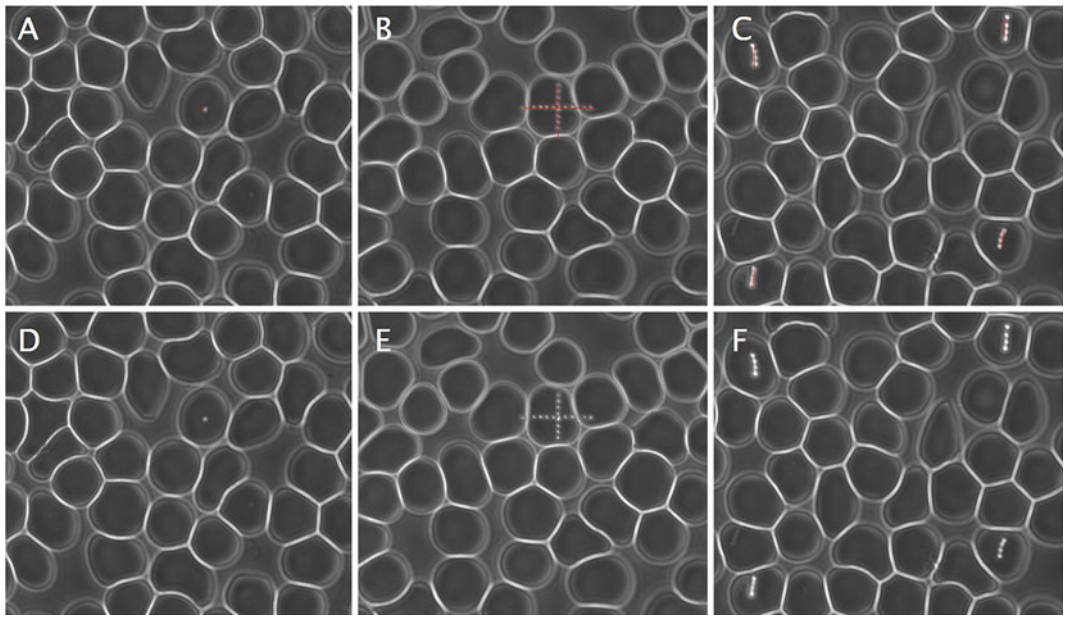

Fig. 5 (**a**) Point spot ablations on RBCs to calibrate targeting. (**b**) Intersected line cuts used to calibrate tilt. (**c**) Four line cuts at each corner to calibrate steering. Figures (**d**)–(**f**) show the ablated RBCs without line cut overlay

4. Fire the laser by clicking "CUT ROI" button under the "Laser Scissors" tab and acquire a new image by clicking "Expose" button under the "Image Acquisition" tab.
5. There will be a new bright dot displayed in the acquired image. It may not be underneath the crosshair.
6. Click "Advanced" under "Operation Mode" tab to access the laser offset parameters in the "Laser Scissors" tab.
7. Adjust the "x offset" and "y offset" parameters to redirect the laser to the crosshair position. Fire at the RBC cells with new offset parameters and acquire image. Repeat process until the bright dot is shown under the crosshair (Fig. 5a).
8. Draw one long horizontal and one vertical line passing through the crosshair, and acquire image to see if there is a tilt horizontally or vertically. If yes, change the values in "x Tilt" and "y Tilt" and repeat process until the two lines are straight (Fig. 5b).
9. Draw lines in the four corners and see if the bright lines overlie with the lines. If not, change the value in "Steer X" and "Steer Y" and repeat process until the targeting is accurate (Fig. 5c).
10. Reduce the laser power to a level that only a very small damage spot can be detected in the RBC. Move the z focus up and down using the yellow button under "Stage Ctl" tab. The difference between the firing z position to the position with the sharpest dot is the z offset. The value can be saved under "Cut ROI."

3.4 Nerve Regeneration: Live Cell Imaging

To perform live imaging of neuronal cells for extended periods of time, the temperature, humidity, and CO_2 concentration of the environment should be controlled. We use a microscope incubator that maintains the proper environment (37 °C, 5 % CO_2) on an inverted microscope.

1. Load the cells onto the microscope and determine the laser threshold for axotomy and sub-axotomy for neuron cells (*see* **Note 8**). The amount of power necessary to create sub-axotomy will vary depending on the laser used. Start by targeting a nerve axon at a low laser power and gradually increase the laser dose until visible thinning of the axon can be seen within a second after laser exposure (Fig. 6). Repeat on several axons to determine the laser dose thresholds for sub-axotomy lesions. Cells may be observed under phase contrast, differential interference contrast (DIC), or fluorescence microscopy.
2. Once the sub-axotomy threshold is determined, look for established growth cones that have active filopodia and lamellipodia. Typically, we use cell cultures 3–5 days post dissection. During this period nerve cultures are actively growing and growth cones are easily identifiable.

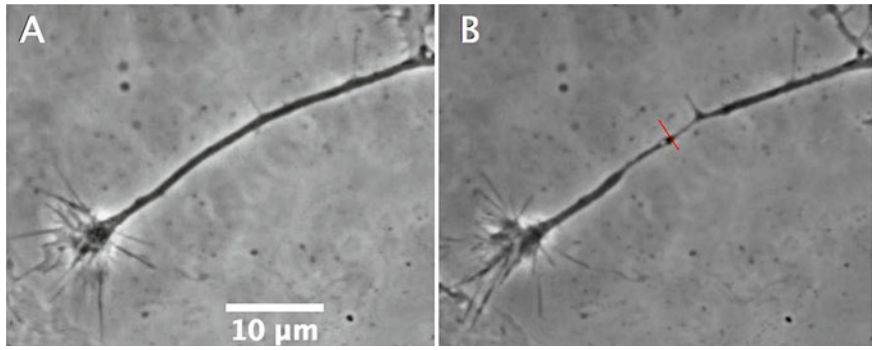

Fig. 6 Hippocampus thinning after laser damage. Growth cone can be found by looking for structures at the end of nerve axons: lamellipodia can be distinguished by the actin network formed at the leading edge. The slender protrusions that extend outward past the lamellipodia are the filopodia

3. Follow and record phase contrast images (or using other forms of microscopy) of the neuron prior to laser ablation to characterize pre-irradiation morphology and behavior. This will be used for the analysis of the growth cone dynamics before laser axotomy.
4. Measure the distance from the growth cone and cell body to the targeted damaged site. The relative position of the cut may affect the dynamics of the repair process. *See* **Note 9**.
5. Damage axon and follow cells by phase contrast images (or other microscopic imaging methods) immediately after damage for up to 60 min. *See* **Note 10**.
6. Compile and analyze phase contrast images from pre and post laser exposure using ImageJ. After laser ablation, phase contrast images showed a visible thinning of the nerve axon followed by a distinct repair process involving cytoskeletal remodeling. The growth cone retracted toward the damage site, possibly providing cytoskeletal material to repair the injured region of the axon. In severely damaged axons, the growth cone retracted past the damaged site and did not recover. The observed retraction may be initiated through the release of chemotrophic factors from the damage site, and which initiate axonal repair [4]. In some neurons, lamellipodia formed at the damage site, or near the cell body traveling toward the damage site probably to assist in the repair of the injured axon (Fig. 7).

   This repair process is consistent with results seen by Difata et al. using a UVA laser to damage hippocampus neurons [11]. After axonal recovery, the nerve cell proceeds to form an apparently normal new growth.
7. Qualitatively score nerve repair based on axonal recovery and growth cone reformation. A "++" score is given to nerve cells that exhibited both axonal repair and growth cone reformation,

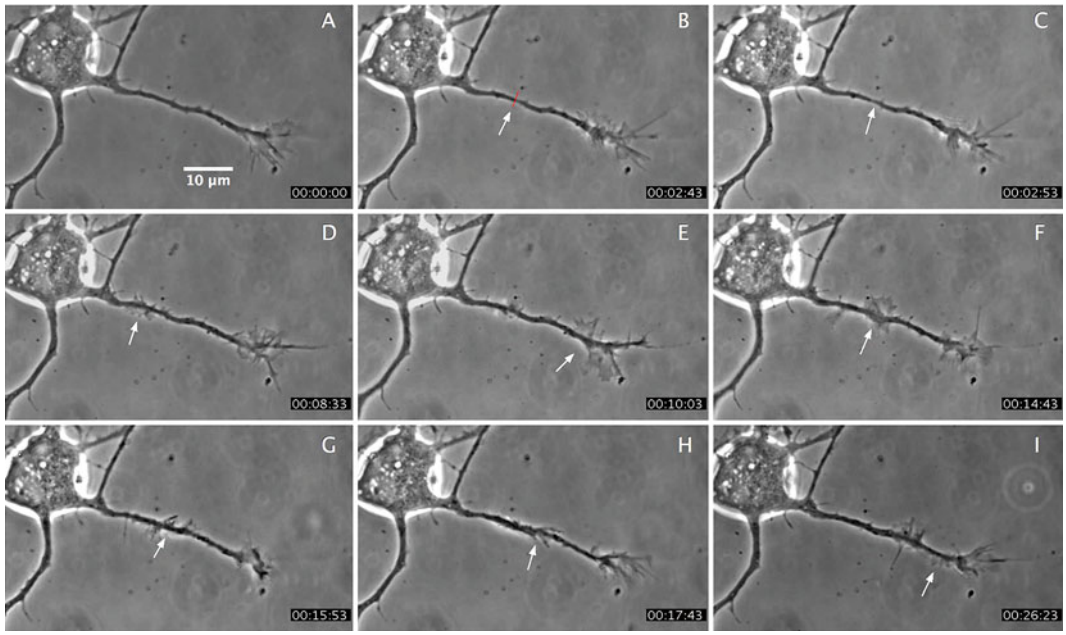

Fig. 7 (**a**) Growth cone before laser sub-axotomy. (**b**) The axon is damaged along the *red line* causing a thinning of the axon. (**c**, **d**) Axon is slightly thinner at ablation site and actin accumulates at the base of the cell body. (**e**) Growth cone retracts slightly and sends repair material toward damage site. (**f**) The growth cone is reduced in size and actin is accumulated at the damage site. (**g**, **h**) Nerve axon thickens and is repaired. (**i**) Lamellipodia progress forward and combines with the growth cone

"+" is given to nerve cells that exhibited axonal repair with partial or no reformation of growth cone, and "−" is given to nerve cells that did not recover from laser damage. In our experiments with hippocampus neurons 24 % of the cells exhibited a "++" response, 29 % showed a "+" response, and 47 % of the neurons did not recover from the laser damage (Table 1).

The laser damage mechanism has not been fully characterized, and may be a combination of single or two photon absorption, or possibly the creation of a plasma and shock wave, all of which likely affect the axon cytoskeletal complex [4]. The axonal thinning produced with the 532 nm ps green laser beam was similar to that observed using a 532 nm ns laser on goldfish retina neurons. Electron micrographs of the retina cells ablated with 532 ns laser showed that the damage did not rupture the cell membrane (Fig. 8).

It appears that the thinning is a result of loss of cytoskeletal structure in the axon even though there was evidence of microtubules in the damage area. However, it is not clear whether or not the microtubules were normal, as they appeared somewhat compressed as viewed in the electron micrographs.

8. To visualize microtubule damage after laser sub-axotomy, transduce nerve cells with red fluorescent protein (RFP) tubulin.

Table 1
Hippocampus neurons

Response	Number	Percent
+	5	29
++	4	24
–	8	47
Total	17	100

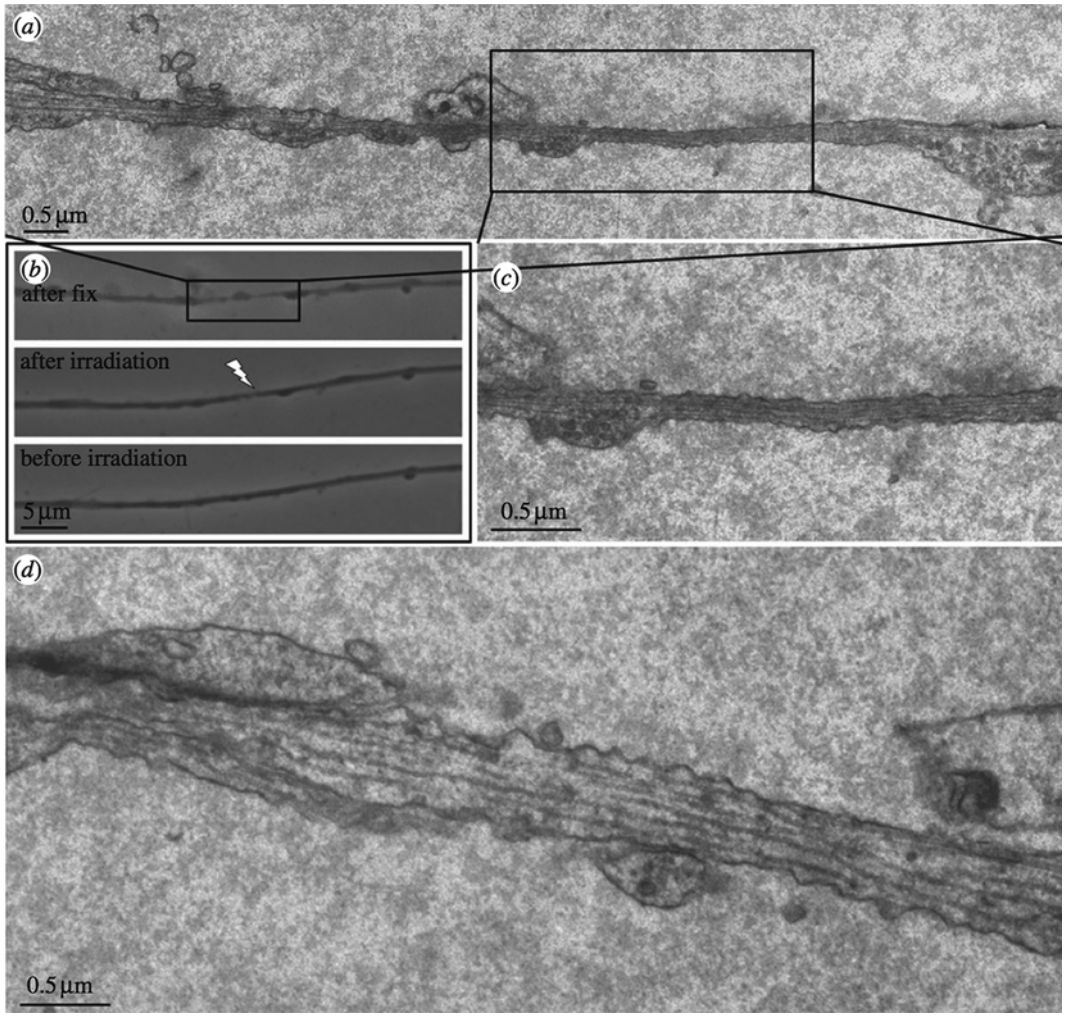

Fig. 8 TEM and phase contrast images of damaged axon: (**a**) reconstructed collage of multiple TEM images of an axon fixed 30 s after laser irradiation. (**b**) Live phase contrast images taken before (*bottom*) and after irradiation (*middle*) and after fixation (*top*). Images are matched with the electron microscope images in (**a**). (**c**) Electron micrograph of the region in the center of the "thinned" zone. Note the intact cell membrane and the presence of contiguous microtubules. (**d**) Non-irradiated region 36 mm away from the laser-irradiated region (Wu et al. [4]). Reprinted from [4] with permission from the Royal Society Interface

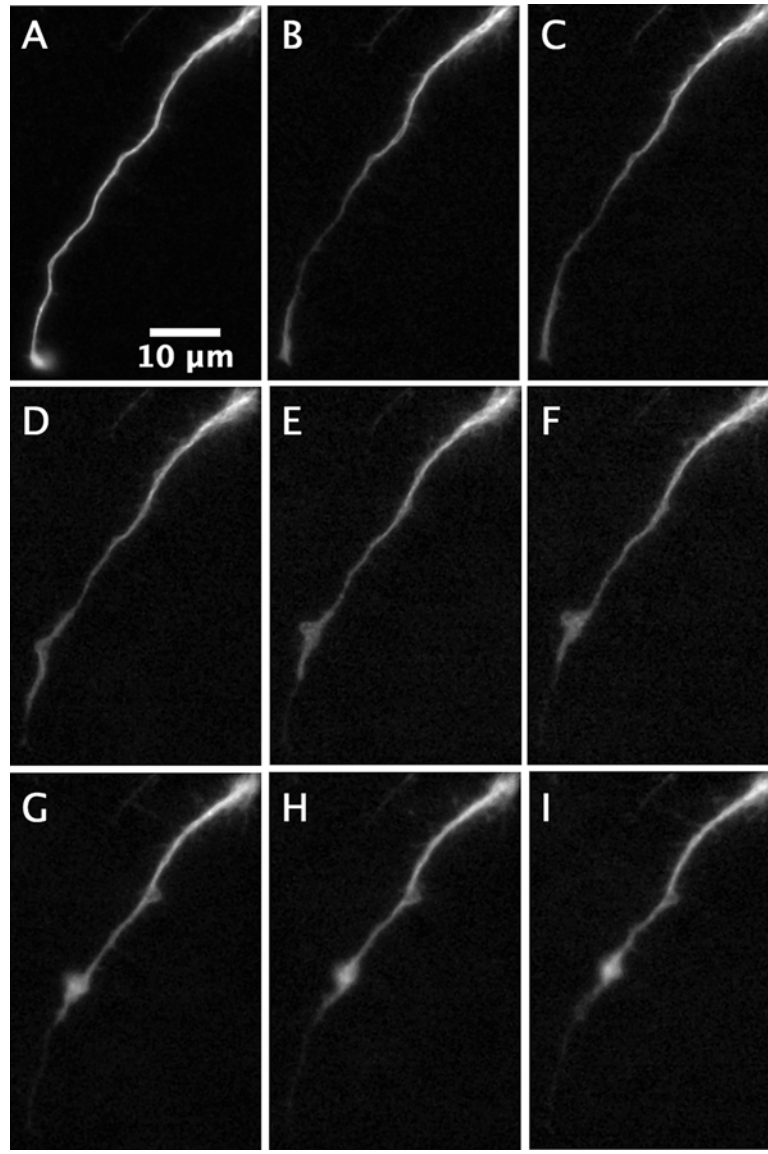

Fig. 9 Hippocampus neuron transduced with GFP tubulin before and after laser radiation

Fluorescence time series analysis showed a visible retraction and accumulation of tubulin at the damage site consistent with the response seen in phase contrast images (Fig. 9).

RFP tubulin signal decreased in intensity at the ablation site, but recovered in intensity as axonal repair proceeded. The fluorescent signal at the damage site indicates microtubule structure was partially preserved after laser sub-axotomy. The decrease in signal is likely due to the microtubule damage seen in electron micrograph.

In summary, we have described a robotic laser microscope that can be used to target axons and create sub-axotomy lesions. The repair process can be studied at the level of individual axons. Additional studies should be done to study the biochemical pathways involved in growth cone sensing and cytoskeletal remodeling. Lasers provide a novel way to study growth cones and their possible role in neuronal repair and regeneration.

4 Notes

1. Selection of the laser for the RoboLase, or any other system should be based on the desire to produce cellular damage using multiphoton process produced by short-pulsed lasers.
2. We have found that some nerve cultures do not grow well on 35 mm dishes. Nerve cell cultures can also be prepared on glass coverslips and placed in culture dishes for imaging.
3. Most laser-related eye injuries occur during laser alignment. When designing optical hardware, try to direct the laser path in such a way that it is not at eye level. Follow all safety procedures and always wear protective eyewear.
4. The transmission factor provided by the manufacturer may vary slightly between lenses and can degrade with usage and time. Thus it is important to measure transmission through the entire system periodically, preferably weekly, but certainly monthly. If multiple people use the system, transmission and alignment should be checked daily and even between different users of the system.
5. Measure power at incremental changes to the polarizer position. This power reading should be done periodically since laser power may fluctuate between experiments.
6. The blood smear is prepared by holding a standard microscope slide at a 45° angle to the cover glass, and while exerting a slight pressure down, sliding the edge of a standard microscope slide through a small drop of human blood. This is a standard "smear" method used in pathology/hematology labs and can easily be mastered.
7. The calibration method shown on the RoboLase system serves as an example. Target calibration can be done differently depending on the software used to control the laser ablation.
8. Start at the RBC threshold and gradually increase power. We have found line cuts work better than point cuts to create laser sub-axotomy.
9. In our experience, we make laser ablations 10–20 μm from the growth cone to get the most consistent response.

10. The repair process can range from 10 min to over 40 min. A frame rate of 10 s was used to capture the growth cone dynamics. Image processing was used to quantify the behavior of the growth cone.

References

1. Tom VJ, Steinmetz MP, Miller JH et al (2004) Studies on the development and behavior of the dystrophic growth cone, the hallmark of regeneration failure, in an in vitro model of the glial scar and after spinal cord injury. J Neurosci 24:6531–6539
2. Erturk A, Hellal F, Enes J et al (2007) Disorganized microtubules underlie the formation of retraction bulbs and the failure of axonal regeneration. J Neurosci 27:9169–9180
3. Bradke F, Fawcett JW, Spira ES (2012) Assembly of a new growth cone after axotomy: the precursor to axon regeneration. Nat Rev Neurosci 13:183–193
4. Wu T, Mohanty S, Gomez-Godinez V et al (2011) Neuronal growth cones respond to laser-induced axonal damage. J R Soc Interface. doi:10.1098/rsif.2011.0351
5. Wu T, Nieminen TA, Mohanty S et al (2012) A photon-driven micromotor can direct nerve fibre growth. Nat Photonics 6:62–67
6. Botvinick EL, Berns MW (2005) Internet-based robotic laser scissors and tweezers microscopy. Microsc Res Tech 68:65–74
7. Berns MW, Botvinick EL, Liaw L et al (2005) Micromanipulation of chromosomes and the mitotic spindle using laser microsurgery (laser scissors) and laser-induced optical forces (laser tweezers). In: Cell biology: a laboratory handbook. Elsevier Press, Burlington, MA
8. Shi L, Berns MW, Botvinick EL (2008) RoboLase: internet-accessible robotic laser scissor and laser tweezers microscope system. Medical Robotics, I-Tech Education and Publishing. ISBN 978-3-902613-18-9
9. Misawa H, Koshioka M, Sasaki K et al (1991) Three-dimensional optical trapping and laser ablation of a single polymer latex particle in water. J Appl Phys 70:3829–3836
10. Gomez-Godinez V, Wu T, Sherman AJ (2010) Analysis of DNA double-strand break response and chromatin structure in mitosis using laser microirradiation. Nucleic Acids Res 38:e202
11. Difato F, Tsushima H, Pesce M et al (2011) The formation of actin waves during regeneration after axonal lesion is enhanced by BDNF. Sci Rep 1:183